

CORROSION BEHAVIOR OF THE FERRITIC STEEL IMPROVED BY COATING IN LIQUID LEAD

¹Lucia ROZUMOVÁ, ¹Martina PAZDEROVÁ, ²Lukáš KOŠEK

¹Research Centre Řež s.r.o., Husinec – Řež, Czech Republic, EU, <u>lucia.rozumova@cvrez.cz</u> ²University of Chemistry and Technology Prague, Technická 5, Prague, Czech Republic, EU

https://doi.org/10.37904/metal.2025.5128

Abstract

Among the advanced reactor designs of the fourth generation of nuclear reactors, the Lead-cooled Fast Reactor (LFR) stands out as one of six distinct types. The corrosion damage of the steels, it is caused by liquid metal acting on the structural material, which is considered a significant obstacle in the development of the fast reactors concept. The corrosion resistance and chemical compatibility with environment of 9Cr-1Mo, ferritic alloy steel (T91), in condition of the static liquid lead with 1.10-6 wt.% oxygen at 520 °C are analysed in this study. The specimens were exposed for 3500 hours. The specimens tested were the reference T91 and T91 with the coating on base Al and Ti was applied to the second specimen. The coating applied by physical vapor deposition were used for corrosion resistance improvement. The formed oxide scale of reference T91 consists of an outer layer with a Fe-Cr spinel structure and an inner internal oxidation zone (IOZ). Corrosion damage was characterized using electron microscopy techniques, which identified networks of solution-based attack (SBA) intrusion beneath liquid lead wetted surfaces. The damage to the coating depends on their chemical composition and structure of the coating. However, in general, the application of the coating increased the resistance of the surface to corrosion damage.

Keywords: Ferritic steel, 9Cr-1Mo, coating, liquid/molten lead, lead-cooled fast reactor (LFR)

1. INTRODUCTION

The escalating global demand for energy and the depletion of conventional fossil fuels, demands new clean energy technologies with high efficiency. One promising energy generation system is a new generation of nuclear reactors (Gen IV). The nuclear power appears as a mature, cleaner alternative gaining widespread recognition and social interest [1,2,3]. Gen IV nuclear reactors belong to nuclear reactors with different operating principles, which share higher safety features and efficiencies than the current reactors. Lead-cooled fast reactors (LFR) represent an innovative concepts of GEN IV reactors. The heavy liquid metals (HLM), namely Pb and Pb-Bi eutectic metals, are excellent cooling media for these types of nuclear reactors. [4,5,6]. The environmental compatibility of structural materials is the key factor limiting the development and application of LFR. However, most of structural materials considered for use in these nuclear systems suffer from considerable general damage in contact with the liquid metals. Full knowledge on compatibility of these structure materials with the coolant is essential for further design and long-term safety operation perspective of HLM-cooled systems [2,6,7].

The 9–12% Cr Ferritic/Martensitic (F/M) steels, such as T91 (a typical F/M steel), have been selected as one of the main candidate structural materials. These materials are considered highly favorable choices for fuel cladding materials and heat exchanger in LFR, because of their high tensile strength, good high-temperature performance, radiation swelling resistance, and thermal conductivity [8,9,10]. The susceptibility of the F/M steels to corrosion when exposed to liquid lead is significantly influenced by the concentration of dissolved oxygen and the surrounding temperature [6,13]. However, it has been observed that these steels demonstrate



high susceptibility to Liquid Metal Corrosion (LMC), exhibiting either severe oxidation or dissolution corrosion depending on the oxygen concentration within the liquid lead [11,12,13,14]. Generally, when the oxygen concentration is lower than 1.10⁻⁸ wt.%, dissolution corrosion is likely to occur, the alloy components, Fe, Cr, and Ni, in the steel matrix are dissolved into liquid lead until the corresponding saturation is reached. When the oxygen concentration is higher around 1.10⁻⁶ wt.%, oxygen saturation, oxidation occurs, which means the formation of the outer oxidation layer [6,15,16,17]. The dissolution and oxidation can be prevented by formation of the protective oxide layer using controlled oxygen content in the coolant, probably around 1.10⁻⁷ wt.% and the use of a protective coating is proving to be an effective and possible way of a protecting the steel [18].

The current work mainly investigates the corrosion behavior of T91 steel and T91 with coating in static liquid lead at 520 °C, aiming to explore its corrosion behavior, corrosion mechanism and functionality of the coating.

2. EXPERIMENTAL

2.1. Material

F/M steel T91 was used for the experiment. Their chemical composition is shown in **Table 1**. and their microstructure of the surface in **Figure**. The Cr–Mo–Mn-V-Nb FM steel T91, heat No. 41.305, was delivered as 91-mm-diameter rod, that had been heat treated at 1030 $^{\circ}$ C/1 h + 680 $^{\circ}$ C/4 h and subsequently air cooled [19].

Table 1 Nominal composition of T91 steel (wt. %)

Steel	Fe	Cr	Мо	Ni	С	Si	Mn	Р	S	Al	Cu	Nb	Ti	V	N
T91	Bal.	10.1	0.88	0.034	0.12	0.39	0.36	0.011	0.002	0.005	0.041	0.052	0.007	0.22	0.065

2.2. Coating

F/M steel T91 was used as a reference material and one coating was applied on the reference material to improve the resistance to HLM environment. The coatings were prepared by Physical Vapour Deposition (PVD) and the composition of the coatings was chosen to ensure the material's ability to form a protective layer and minimize oxidation of the base material. Coating MARWIN was on nanoscale base AlTiN, which was formed by a layer with a continuous change in composition. Surface morphology of the coating can be seen in **Figure 1.**

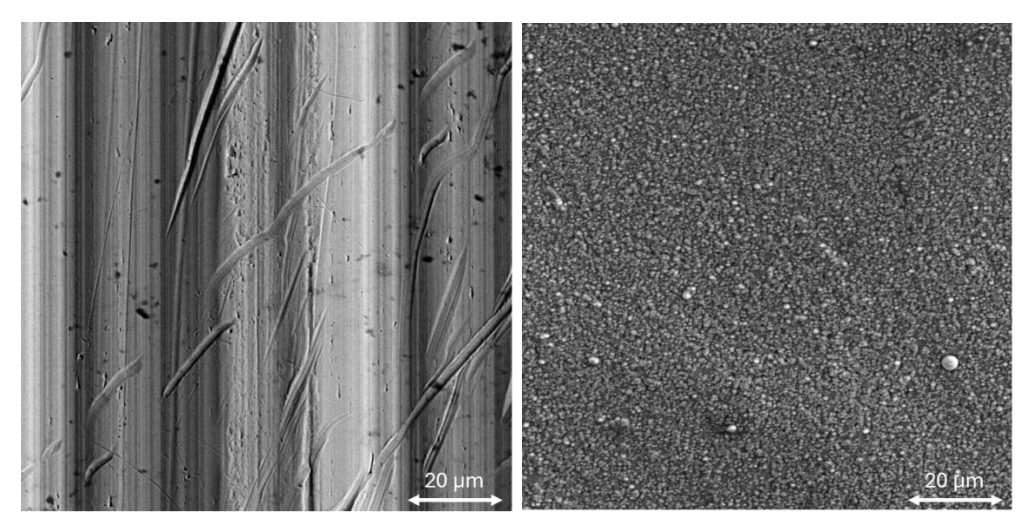


Figure 1 SEM-BSE surface morphology of the original surface of the test specimen: T91 as rec. (left) and T91+MARWIN (right)



2.3. Specimens

For the experiment was used the corrosion coupons. The dimensions of the tested specimens were 20 x 5 x 1.5 mm. Before exposure, all specimens were ultrasonically cleaned with acetone and dried.

2.4. Experimental procedure

An instrumented static tank was used for experiments with liquid lead, as can we have seen in Figure 2. Static tank consists of a 4.5 I stainless-steel test chamber. Inside the static tank is embedded an alumina (Al₂O₃) crucible. This crucible prevents the direct contact of the steel walls with the Pb during the exposure. Onto the chamber outer surface are reeled the heating elements, which allow the melting at the lead and controlling the test temperature. The whole setup is thermally insulated. The thermal insulation of the whole setup minimizes potential heat losses. The high temperature of the lead ensures gradient in the liquid lead bath. The static tank has the airlock and the test chamber which separates from each other a ball valve. The airlock chamber is used for vacuuming of the specimens in an inert gas atmosphere. The vacuuming is being carried out before and after their immersion into the liquid metal to avoid oxidation during heating up and cooling down. For testing at static conditions was used a simple immersion method. The specimens in holder were vacuumed by pure argon in the test chamber. The lead was heated up to 520 °C to melt. After the melt stabilization and adjustment of the oxygen concentration, the holders with the fixed test specimens were immersed from the air-tight air-lock chamber into the liquid lead. A reducing Ar+H₂ (6 %) gas mixture was used as a cover gas. The automatic gas mixing was used to ensure the required oxygen concentration values (Ar+H2 (6 %) with Ar+O₂ (10 %)). The oxygen concentration maintaining in the lead at the target level was used the active oxygen control. This was based on the oxygen sensor signal measurement. Oxygen sensors based on the Bi/Bi₂O₃ reference electrode were used.

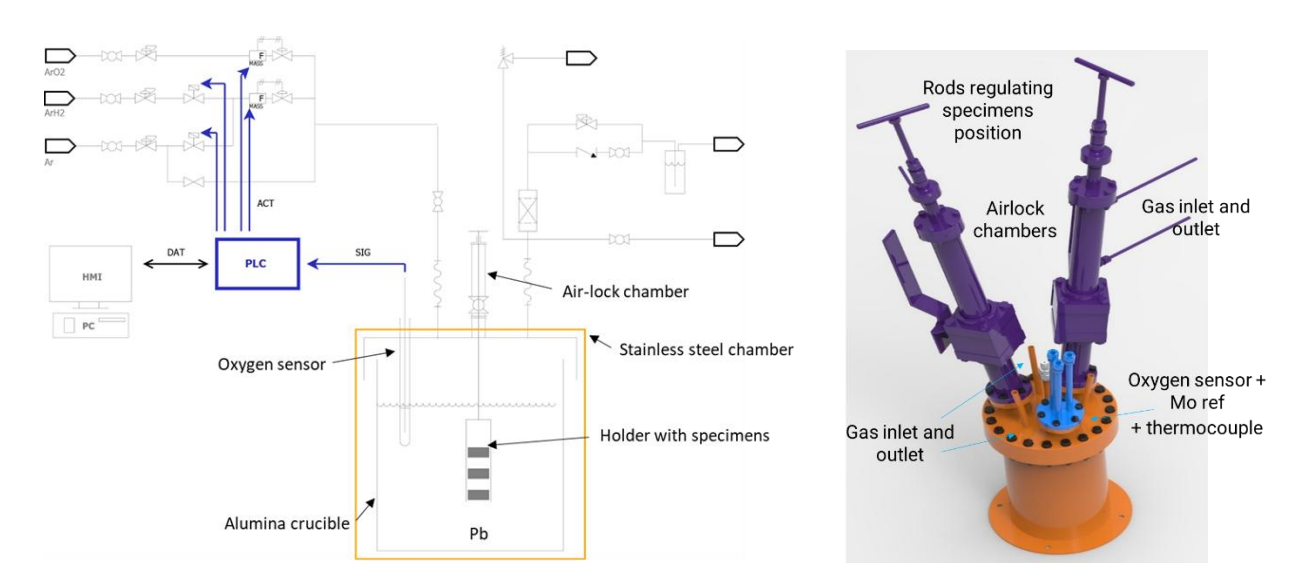


Figure 2 Scheme of experimental setup (left) and 3D layout of static tank (right)

The prepared specimens were made in liquid lead for 3500 hours with high oxygen concentration 1.10⁻⁶ wt.%. After exposure, the specimens were observed on the surface and after that they were metallographically cut for cross section analyses. This process was followed by the analysis and thickness measurements of the oxide layer and for specimens with a coating, the resistance of the coating was evaluated from the point of view of the protection of the base material. The evaluation of the surface layers was carried out using a Scanning Electron Microscope (SEM, LYRA3 and MIRA 3 TESCAN) equipped with detectors for the imaging of Backscatter Electrons (BSE) and Energy Dispersive Spectroscopy (EDS) for chemical analysis.



3. RESULTS AND DISCUSSION

Post test observation by SEM showed large differences between coated and uncoated specimens. The corrosion mechanism of the tested uncoated materials can be defined as a combination of the double oxide layer formation and solution-based attack (SBA) with penetration of lead to the base material (Figure 3). Outer oxidation of T91 steel was found almost over the entire surface of the specimens (99 %). Outer oxide layer was homogeneous and compact, and it is composed from iron oxides. This outer oxide layer was not protective, and did not prevent the formation of inner oxide, SBA, and Pb penetration into the base material. Double inner oxide layer was observed on 100 % of the surface area. This inner layer was composed from mixed oxide Fe-Cr-O. The layer that was closer to the surface was depleted by Cr and the part closer to the base material, below it, was richer by Fe. Maximum depth of the inner oxide layer was around 22 µm. Cr content was not sufficient to protect the steel from the SBA, results can be seen in Figure 3. Cross section observation showed very deep solution-based attack (SBA) including lead penetration into the base material. The SBA part reached a maximum deep of 19.3 µm and total affected area reached 20 % from the entire perimeter of the monitored sample.

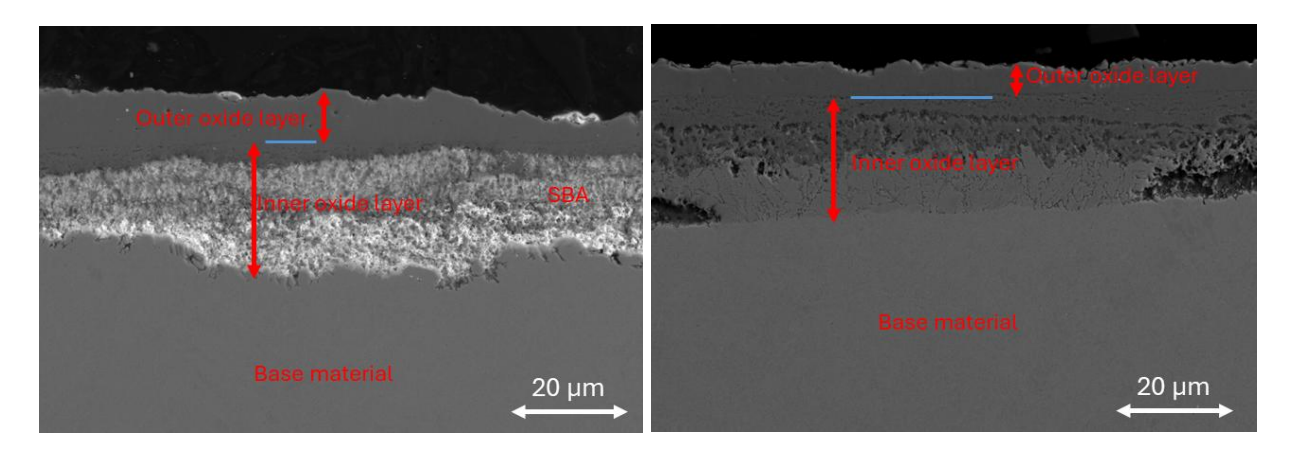


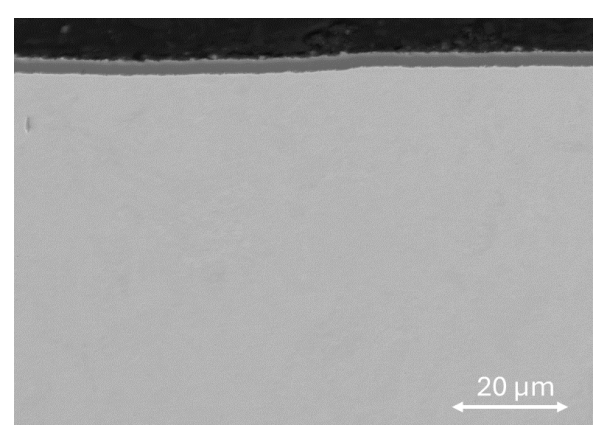
Figure 3 SEM images of T91 steel without coating after 3500 h exposure

The evaluation of the coating after exposure showed that the coating has a stable, uniform, and compact structure without defects. Application of the coatings improved the resistance of T91 steel to the SBA and Pb penetration. As can be seen in **Figure 4**, no SBA was found under the protective coatings. The coating had uniform thickness around 1.9 µm, composed of aluminum titanium nitride (AlTiN). Coating MARWIN were not affected by the exposure. Their structure was sufficiently dense to prevent the penetration of lead through the coating to the base material. The problem arises when there is a defect in the coating, subsequently internal and external oxidation occurs at the defect site, which would likely subsequently cause SBA and penetration of Pb into the base material.

For characterization of the corrosion degradation and determination of the corrosion depth, thirty evenly spaced images were captured along both sides, each having a 100 μ m field-of-view. Ten measurements were acquired from each image. The relative frequency of the corrosion depth was calculated as several data falling into the corresponding interval of depths, divided by the total number of data points (300).

Application of the coatings eliminated the oxidation processes and SBA. Coating MARWIN forms a protective barrier for the steel against oxidation but must not have any defects. Every defect caused immediate oxidation, creation of the inner and outer layer (**Table 2**).





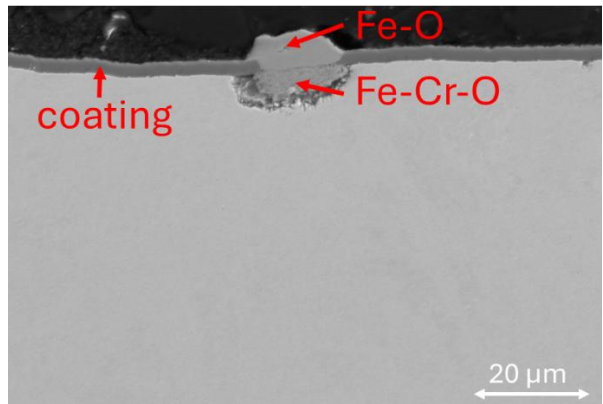


Figure 4 SEM images of T91+MARWIN coating after 3500 h exposure

Table 2 Comparison of the corrosion resistance of T91 steel and protective coating

Specimen	Affected area (%)	Outer oxidation depth avg. / max. (µm)	Inner oxidation depth avg. / max. (µm)	SBA depth avg. / max. (µm)		
T91	100	5.82 / 16.48	15.55 / 21.91	1.48 / 19.31		
T91+MARWIN	15	0.04 / 6.07	0.35 / 9.46	0.03 / 12.93		

4. CONCLUSION

In this paper corrosion resistance of T91 without and with PVD coating was evaluated. The specimens were exposed to liquid lead with high oxygen content for 3500 h.

In conclusion, it can be said that:

- Severe degradation of ferritic martensitic steel without coating SBA, Pb penetration, oxidation.
- High oxygen content and HLM environment is not suitable for T91 steel without protective coating.
- Low Pb penetration and oxidation through the coating.
- The coating forms a protective barrier/layer but must not contain defects.

ACKNOWLEDGEMENTS

This research was funded by the Technology Agency of the Czech Republic (TACR), grant number TK04030082, and the presented results were obtained using the CICRR infrastructure, which was funded by the Ministry of Education, Youth and Sports, grant number LM2023041.

REFERENCES

- [1] MASARI, F., SZAKALOS, P., PETERSSON, C., TORRALBA, J.M., CAMPOS, M. Corrosion and mechanical behavior of novel alumina forming steels in molten lead. *Journal of Nuclear Materials*. 2025, vol. 605, p. 155587.
- [2] ZHU, Z., ZHANG, Q., TAN, J., WU, X., MA, H., ZHANG, Z., REN, Q., HAN, E-H., WANG, X. Corrosion behavior of T91 steel in liquid lead-bismuth eutectic at 550 °C: Effects of exposure time and dissolved oxygen concentration. *Corrosion Science*. 2022, vol. 204, p. 110405.
- [3] ZHOU, Z., DU, J., TIAN, C., PENG, X., WU, Y., LV, X., ZHANG, Y., CHEN, Z. Local mechanical properties of corrosion layers formed on T91 and SS316L steels after exposure to static liquid LBE at 500 °C for 1000 h obtained by nano-indentation. *Nuclear Engineering and Technology*. 2024, vol. 56, pp. 3067-3075.
- [4] PIORO, I.L. Handbook of Generation IV Nuclear Reactors, Elsevier, 2016.



- [5] STANCULESCU, A. GIF R&D outlook for generation IV nuclear energy systems: 2018 update. *Proceedings of the Generation IV International Forum*, Paris, France, 2018, pp. 16-18.
- [6] KOSEK, L., ROZUMOVA, L., HOJNA, A., PAZDEROVA, A. Performance of 9Cr Ferritic-Martensitic Steels in Flowing Lead for 8000 h. *Journal of Nuclear Materials*. 2021, vol. 554, p. 153092.
- [7] KELLY, J.E. Generation IV International Forum: a decade of progress through international cooperation. Progress in Nuclear Energy. 2014, vol. 77, pp. 240-246.
- [8] SORDO, F., ABANADES, A., LAFUENTE, A., MARTINEZ-VAL, J.M., PERLADO, M. Material selection for spallation neutron source windows. *Nuclear Engineering and Design*. 2009, vol. 239, pp. 2573-2580.
- [9] WANG., Li, LIAO, Q. ZHANG, J., LIU, S., GAN, S., WANG, R., GE, F., CHEN, L., XU, S., POLCAR, T., DAGHBOUJ, N., LI, B. Corrosion behavior of Cr coating on ferritic/martensitic steels in liquid lead-bismuth eutectic at 600 °C and 700 °C. *Journal of Materials Research and Technology*. 2024, vol. 29, pp. 3958-3966.
- [10] SCHROER, C., TSISAR, V., DURAND, A., WEDEMEYER, O., SKRYPNIK, A., KONYS, J. Corrosion in Iron and Steel T91 Caused by Flowing Lead–Bismuth Eutectic at 400 °C and 10–7 Mass% Dissolved Oxygen. *Journal of* Nuclear Engineering and Radiation Science. 2019, vol. 5, p. 011006.
- [11] GONG, X., SHORT, M.P., AUGER, T., CHARALAMPOPOULOU, E., LAMBRINOU, K. Environmental degradation of structural materials in liquid lead- and lead-bismuth eutectic-cooled reactors. *Progress in Materials Science*. 2022, vol. 126, p. 100920.
- [12] LAPINGTON, M.T., ZHANG, M., MOODY, M.P., ZHOU, W.Y., SHORT, M.P., HOFMANN, F. Characterization of corrosion damage in T91/F91 steel exposed to static liquid lead-bismuth eutectic at 700–715 °C. *Journal of Nuclear Materials*. 2023, vol. 586, p. 154687.
- [13] HOJNA, A., DI GABRIELE, F., KLECKA, J. Characteristics and Liquid Metal Embrittlement of the steel T91 in contact with Lead Bismuth Eutectic. *Journal of Nuclear Materials*. 2016, vol. 472, pp. 163-170.
- [14] ZHANG, J. A review of steel corrosion by liquid lead and lead–bismuth. *Corrosion Science*. 2009, vol. 51, pp. 1207-1227.
- [15] WANG, W., YANG, C., YOU, Y., YIN, H. A Review of Corrosion Behavior of Structural Steel in Liquid Lead–Bismuth Eutectic. *Crystals*, 2023, vol. 13, p. 968.
- [16] ZHANG, H., Liu, X., XU, Y., ZHAO, L., PENG, T., QIN, C., YU, R., WANG, Z., YAO, C. Comparison investigation on corrosion of SIMP and T91 steels exposed to liquid LBE at 450 °C: The role of Si on reducing oxidation rate. *Corrosion Science*, 2023, vol. 225, p. 111553.
- [17] TIAN, S., JIANG, Z., ZHU, G., LUO, L., LIU, J. Corrosion kinetics of T91 steel under low oxygen conditions (10–7 wt% O) in lead-bismuth eutectic at 500 °C. Materials Today Communications. 2024, vol. 39, p. 109106.
- [18] KOSEK, L., ROZUMOVA, L., HOJNA, A., APARCIO, C., VRONKA, M., VIT, J. Mechanism of localized corrosion issues of austenitic steels exposed to flowing lead with 10⁻⁷ wt.% oxygen at 480 °C up to 16,000 h, *Journal of Nuclear Materials*. 2022, vol. 572, p. 154045.
- [19] BERKA, J. Testování konstrukčních materiálů pro vysokoteplotní plynem chlazené reaktory. *Paliva.* 2013, vol. 5, pp. 136-141.